Energy-independent PWA

of

$$\pi^- p \longrightarrow \Lambda K^0$$

and

$$\gamma p \longrightarrow p\pi^0$$

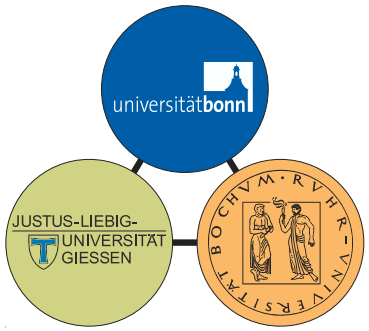

SFB/TR16

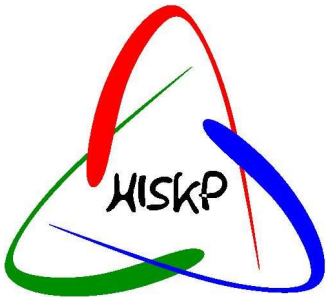

E. Klempt

Helmholtz-Institut für Strahlen– und Kernphysik

Universität Bonn

Nußallee 14-16, D-53115 Bonn, GERMANY

e-mail: klempt@hiskp.uni-bonn.de

7^{th} International Workshop on

PION NUCLEON PARTIAL WAVE ANALYSIS

AND THE INTERPRETATION OF BARYON RESONANCES

20 - 23 September 2013 Camogli (Italy)

Energy-Independent Partial Wave Analysis

1. **Introduction to energy dependent and independent analyses**

   - Status of the Baryon Resonance Spectrum

   - Energy dependent versus energy-independent analyses

2. $\pi^- p \rightarrow \Lambda K^0$

   - Definition of observables

   - Data and fit at low energies ($d\sigma/d\Omega, P$)

   - Data and fit at high energies ($d\sigma/d\Omega, P, \beta$)

   - Truncated fits (with S and P waves)

   - Comparison with Shresta and Manley

3. $\gamma p \longrightarrow p\pi^0$

- Photoproduction amplitudes
- Measurable quantities, and measured ones
- Energy-dependent fits with $L = 0, 1, 2,$ and 3
- What causes the peak in S_{11} and the dip in P_{11} ?
- Results

4. Summary and Conclusions

2 Introduction to energy dependent and independent analyses

2.1 Status of the Baryon Resonance Spectrum

Resonance	Mass	Resonance	Mass	Resonance	Mass
$N(940)$	940	$\Delta(1232)$	1232 ± 1	$N_{1/2^+}(1440)$	1450 ± 32
$N_{1/2^-}(1535)$	1538 ± 10	$N_{3/2^-}(1520)$	1522 ± 4	$N_{1/2^-}(1650)$	1660 ± 18
$N_{3/2^-}(1700)$	1725 ± 50	$N_{5/2^-}(1675)$	1675 ± 5	$\Delta_{1/2^-}(1620)$	1626 ± 23
$\Delta_{3/2^-}(1700)$	1720 ± 50	$\Delta_{3/2^+}(1600)$	1615 ± 80	$N_{3/2^+}(1720)$	1730 ± 30
$N_{5/2^+}(1680)$	1683 ± 3	$N_{1/2^+}(1710)$	1713 ± 12	$\Delta_{1/2^+}(1750)$	
$N_{1/2^-}(1905)$	1905 ± 50	$N_{3/2^-}(1860)$	1850 ± 40	$N_{1/2^+}(1880)$	1870 ± 35
$N_{3/2^+}(1900)$	1905 ± 30	$N_{5/2^+}(1910)$	1880 ± 40	$N_{7/2^+}(1990)$	2020 ± 60
$\Delta_{1/2^-}(1900)$	1910 ± 50	$\Delta_{3/2^-}(1940)$	1995 ± 60	$\Delta_{5/2^-}(1930)$	1930 ± 30
$\Delta_{1/2^+}(1910)$	1935 ± 90	$\Delta_{3/2^+}(1920)$	1950 ± 70	$\Delta_{5/2^+}(1905)$	1885 ± 25
$\Delta_{7/2^+}(1950)$	1930 ± 16	$N_{1/2^+}(2100)$	2090 ± 100	$N_{1/2^-}(2090)$	
$N_{3/2^-}(2120)$	2150 ± 60	$N_{5/2^-}(2060)$	2065 ± 25	$N_{7/2^-}(2190)$	2150 ± 30
$N_{5/2^-}(2060)$	2060 ± 15	$N_{9/2^-}(2250)$	2255 ± 55	$\Delta_{1/2^-}(2150)$	
$\Delta_{5/2^-}(2223)$		$\Delta_{7/2^-}(2200)$		$N_{9/2^+}(2220)$	
$\Delta_{7/2^+}(2390)$		$\Delta_{9/2^+}(2300)$		$\Delta_{11/2^+}(2420)$	
$\Delta_{9/2^-}(2400)$		$\Delta_{3/2^-}(2350)$		$N_{11/2^-}(2600)$	
$N_{13/2^+}(2800)$		$\Delta_{13/2^-}(2750)$		$\Delta_{15/2^+}(2950)$	

(black, grey, light brown: Höhler and Cutkosky, blue new from BnGa, light brown: not seen by GWU)

2.2 Energy dependent versus energy-independent analyses

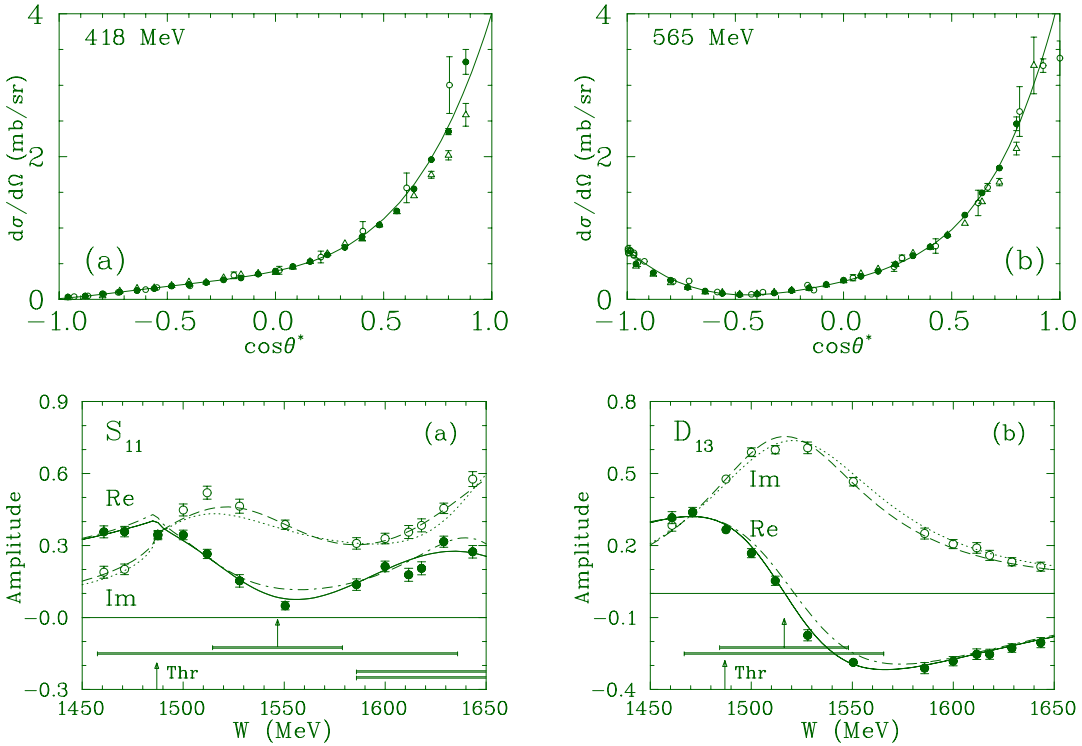

Energy-independent analysis: Fit to single-energy bins to determine real and imaginary part of all partial waves.

Energy-dependent analysis: fit to real and imaginary part of one partial wave with a model OR fit to the experimental data with a model for all partial waves.

3 $\pi^- p \longrightarrow \Lambda K^0$

3.1 Definition of observables, pseudoscalar + octet baryon

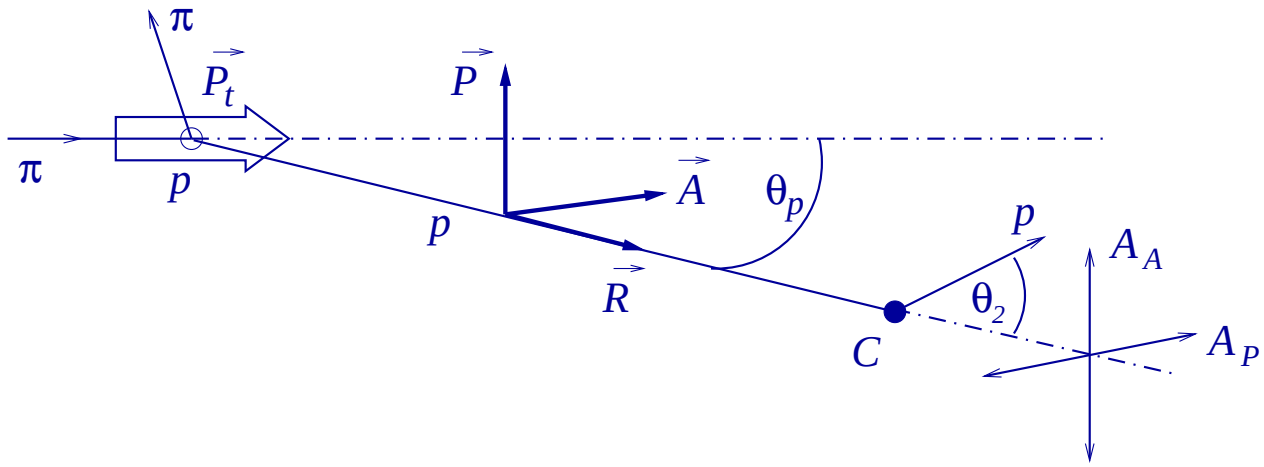

$$\frac{d\sigma}{d\Omega} = \frac{k}{q}(|f|^2+|g|^2)\,,$$

$$(1\pm P)\frac{d\sigma}{d\Omega} = |f\pm ig|^2\,,$$

$$R = \frac{2Re(f^*g)}{|f|^2+|g|^2}\,,\quad A=\frac{|f|^2-|g|^2}{|f|^2+|g|^2}\qquad \tan\beta=-\frac{R}{A}.$$

$$f(W,z) = \frac{1}{\sqrt{qk}}\sum_{l=0}^{L}\left[(l+1)A_l^+(W)+lA_l^-(W)\right]P_l(z)\,,$$

$$g(W,z) = \frac{1}{\sqrt{qk}}\sin\Theta\sum_{l=1}^{L}\left[A_l^+(W)-A_l^-(W)\right]P_l'(z)\,.$$

3.2 Data and fit at low energies ($d\sigma/d\Omega, P$)

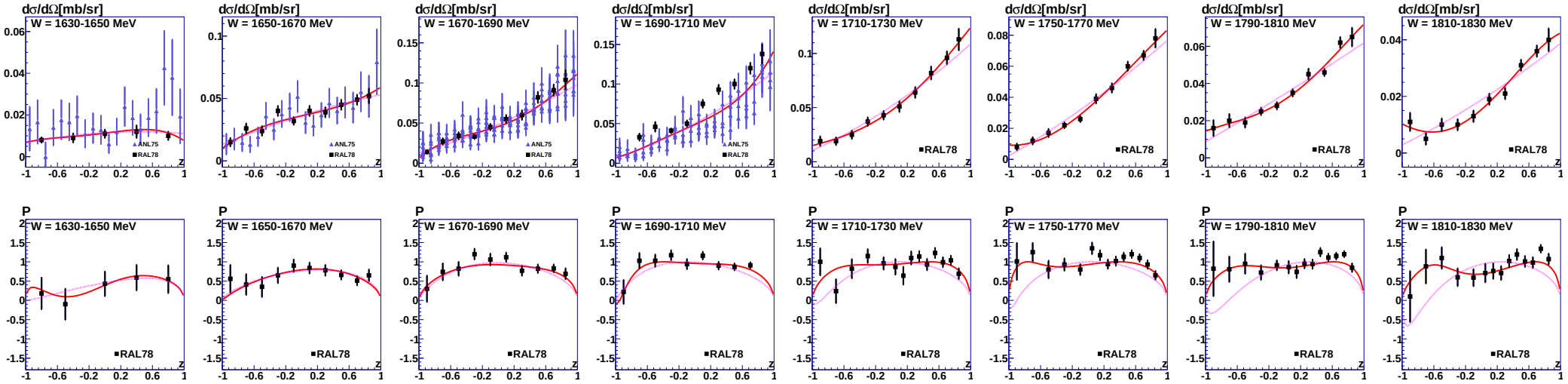

Differential cross sections and Λ polarization for the reaction $\pi^- p \rightarrow K^0 \Lambda$ from ANL75 (blue) and RAL78 (black). The data are compared to two fits using S and P waves (red dotted line) and with S, P and D waves (red solid line).

3.2a Data and fit at low energies ($d\sigma/d\Omega, P$)

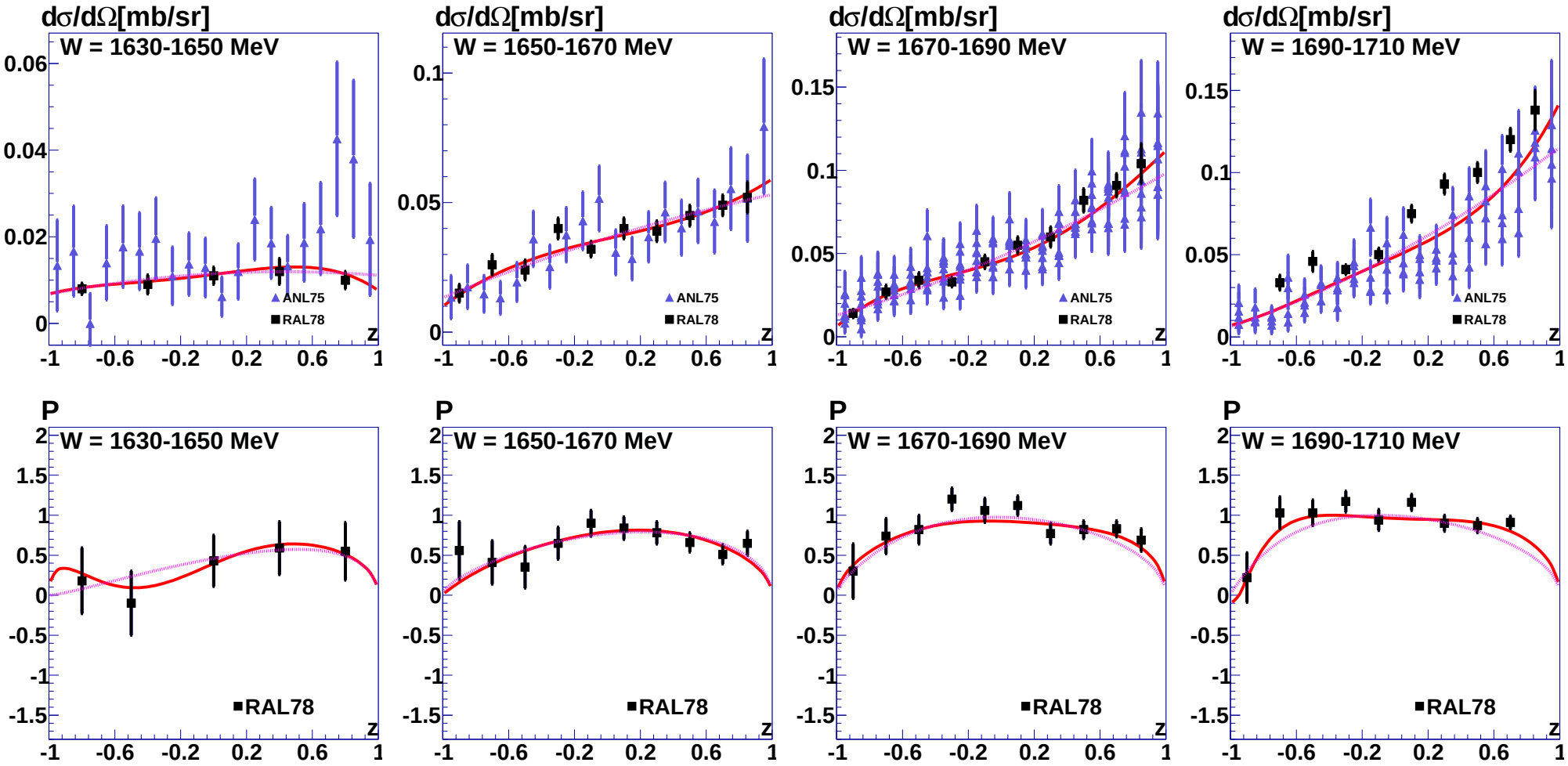

3.2 Data and fit at low energies ($d\sigma/d\Omega$, P)

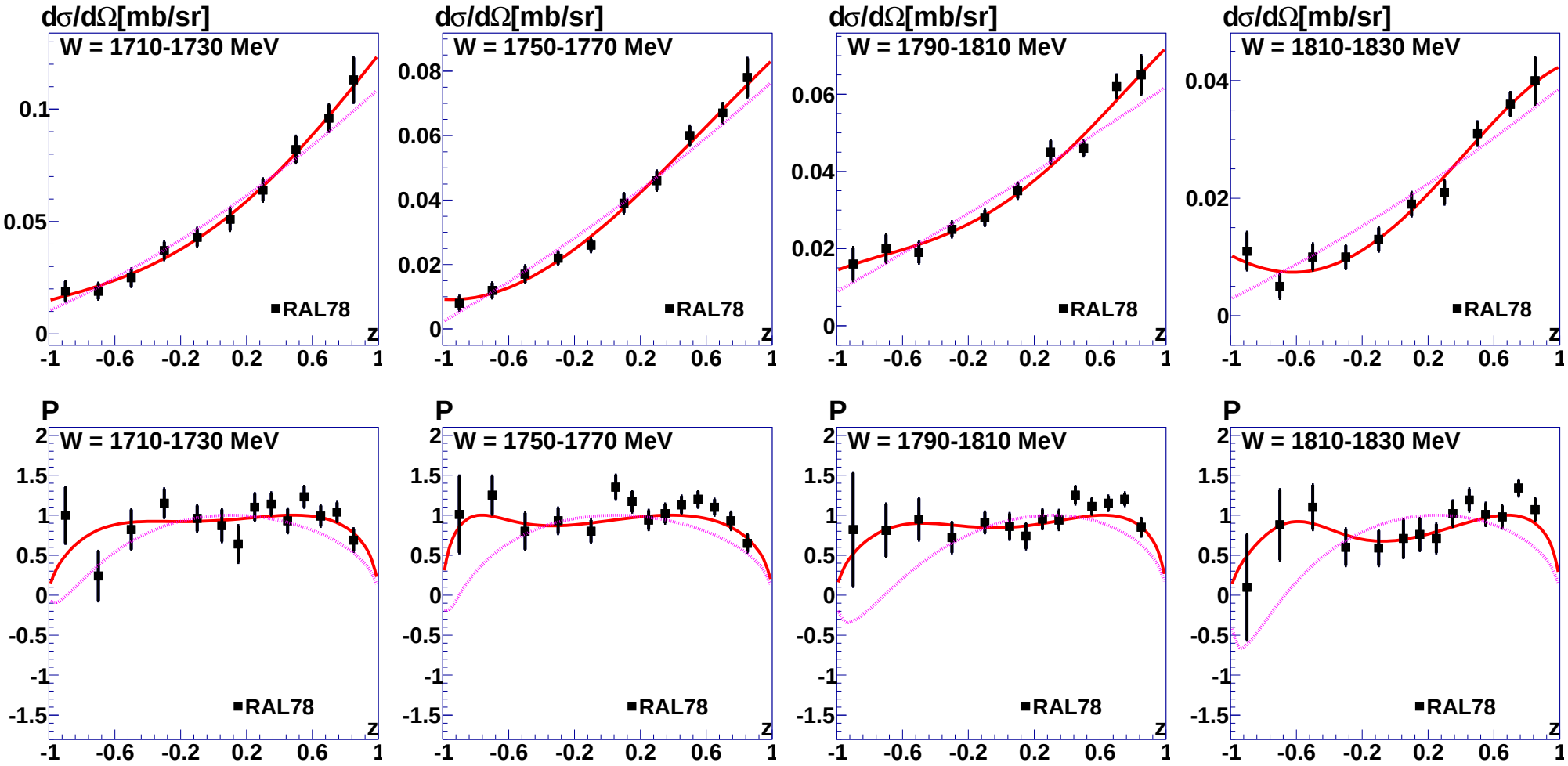

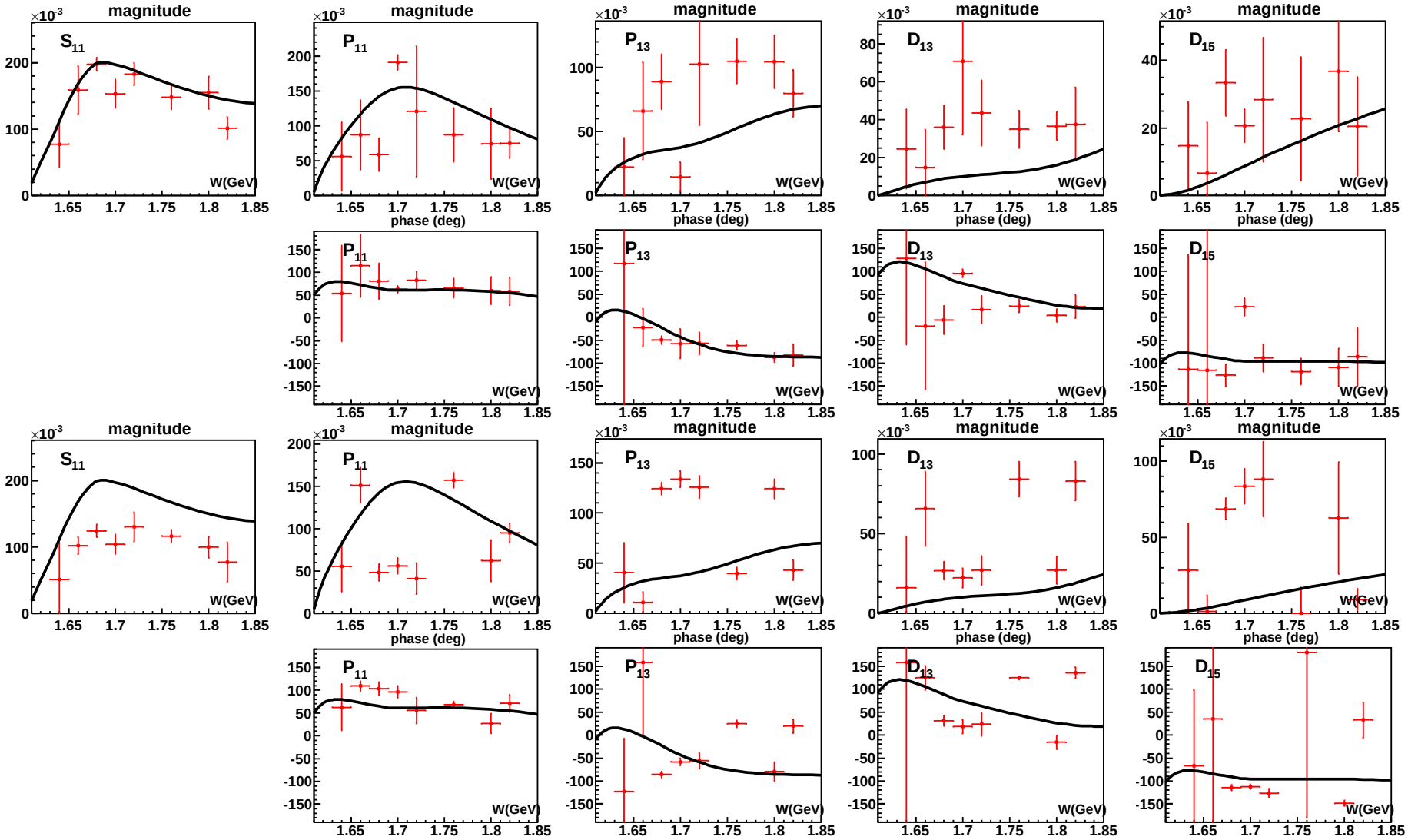

Ambiguous solutions for the decomposition of the $\pi^- p \to \Lambda K^0$ scattering amplitudes with S, P and D waves. The solid line is the energy dependent solution BnGa2011-02. The upper solution is the closest to the energy-dependent fit, it agrees with the BnGa energy dependent fit with $\chi^2/N = 188/72$. The lower solution gives the worst χ^2.

There is a huge number of different solutions!

3.3 Data and fit at high energies ($d\sigma/d\Omega$, P, β)

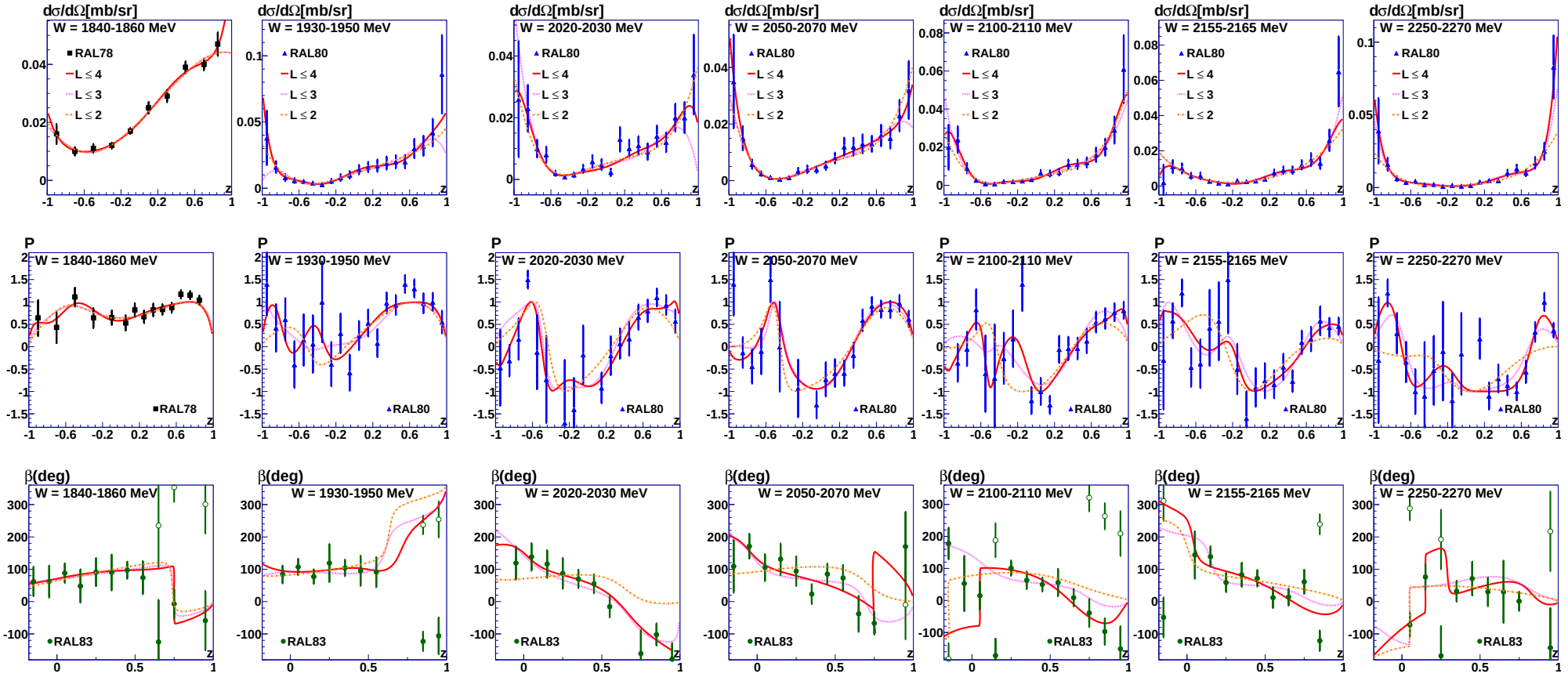

Energy independent fit (red lines) for $\pi^- p \rightarrow K^0 \Lambda$ reaction in the region $1840\text{-}2270$ MeV. The experimental data are from RAL78, RAL80, and RAL83. Note that β is 360-degree cyclic which leads to additional data points shown by empty circles.

Now there is only one solution !

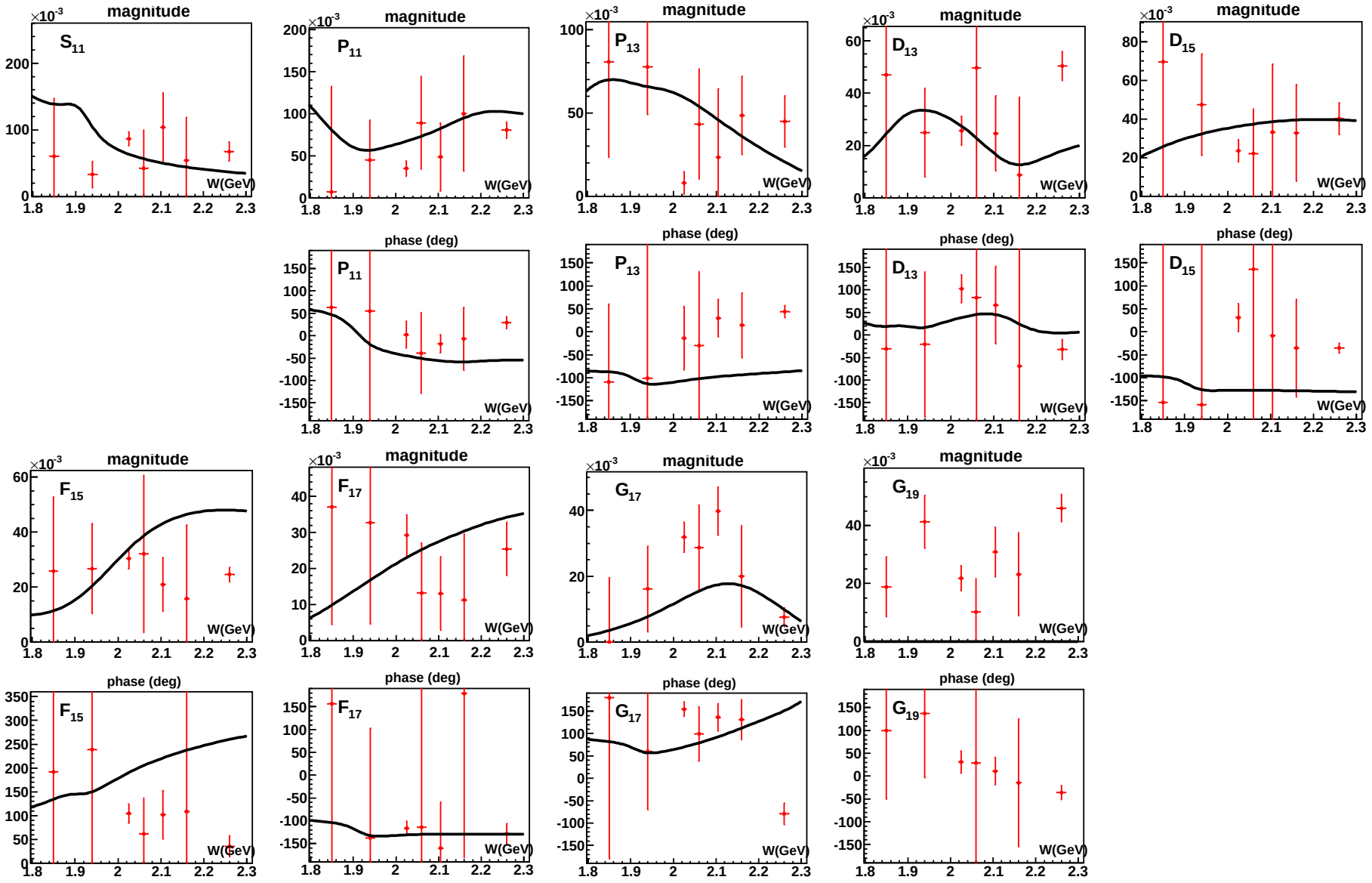

Decomposition of the $\pi N \to \Lambda K$ scattering amplitudes with S, P, D, F and G waves. The solid line is the energy dependent solution BnGa2011-02.

Errors large, not convincing !

3.4 Truncated fits (with S and P waves)

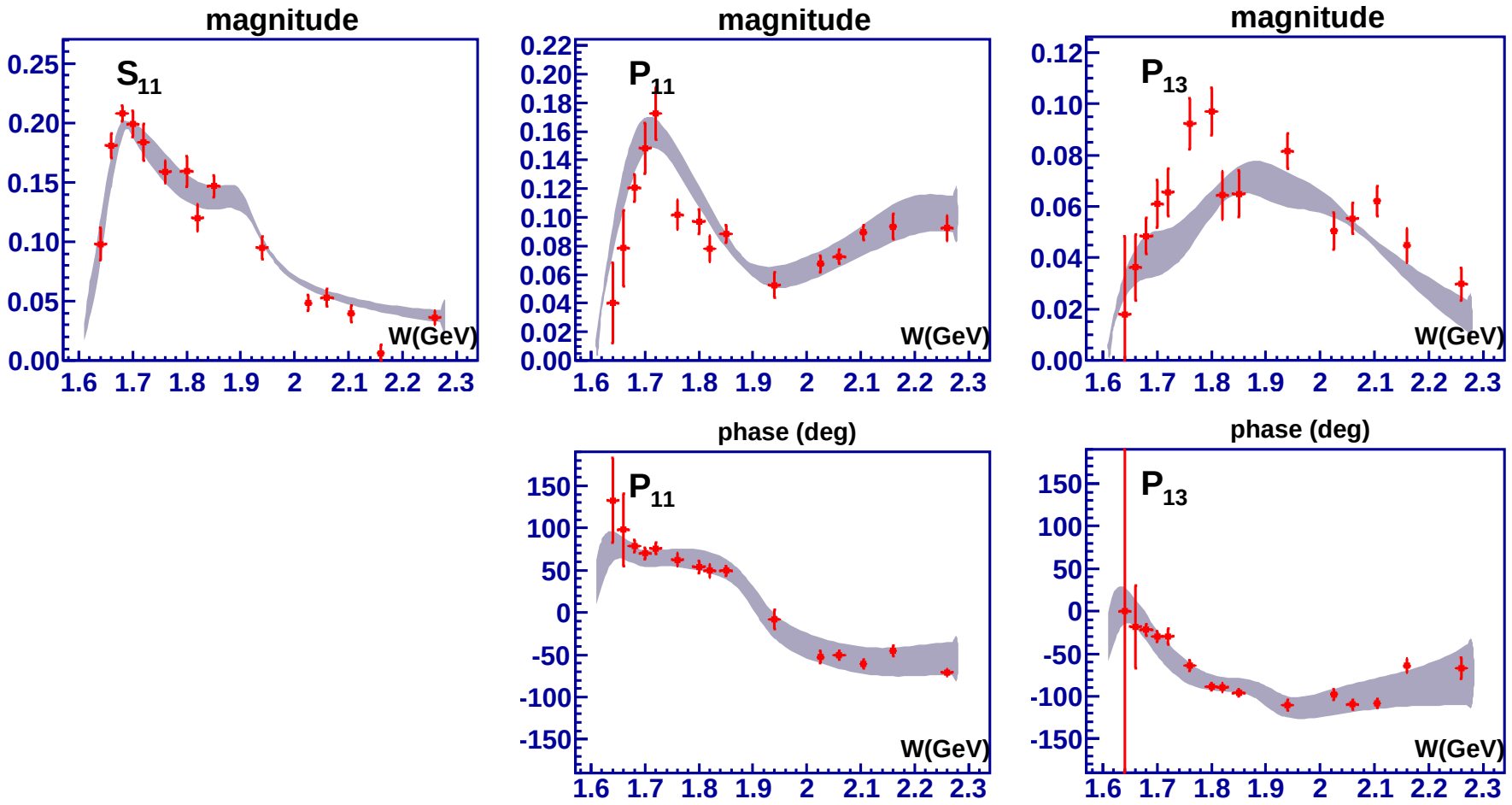

Fit with free S and P-waves and D, F, and G-waves fixed to the energy-dependent solution BnGa2011-02.

"Peak" in P_{13} wave correlated with dip in P_{11} wave and not associated with any phase motion.

3.5 Comparison of Shresta and Manley with BnGa

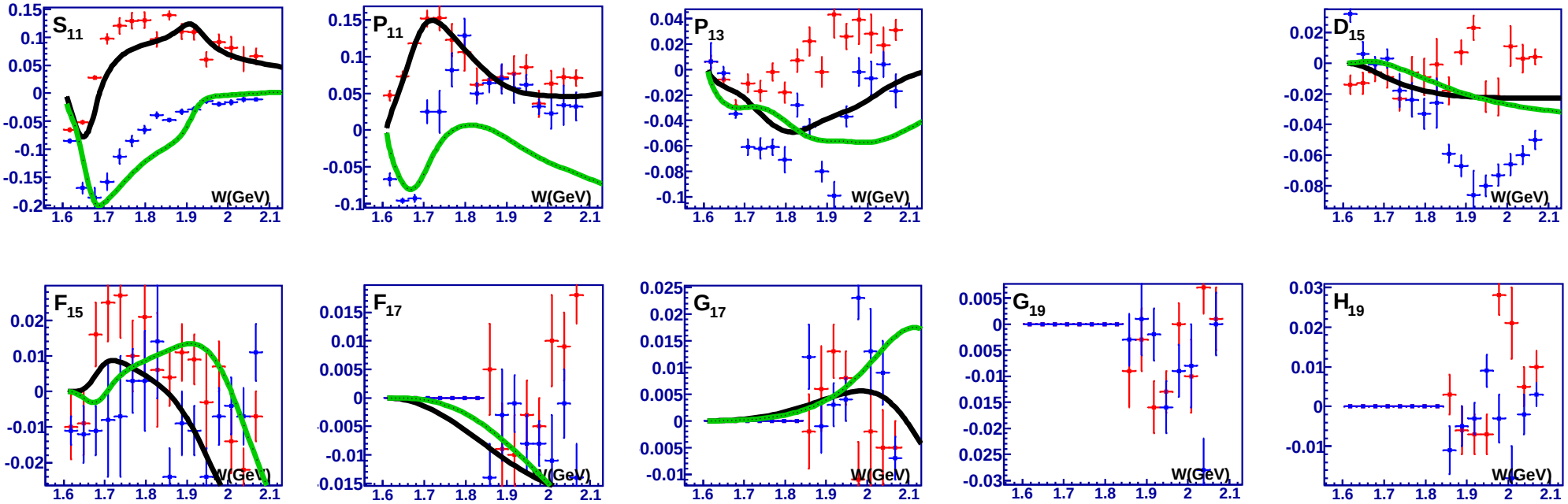

Points with error bars: Single energy analysis of Shresta and Manley. Curves: BnGa2011.

Shresta and Manley start from a model-dependant fit and select the solution of the energy-independent analysis which is closest to the energy-dependent fit. They first freeze the S_{11} wave, then S_{11} and P_{11}, to the energy dependent solution.

Be cautious! The results of an energy-independent (single channel) analysis look like data. They are not!

4 Energy independent analysis of $\gamma p \longrightarrow p\pi^0$

4.1 Photoproduction amplitudes

Four (complex) CGLN amplitudes

$$\mathcal{F} = i\,(\vec{\sigma}\cdot\hat{\epsilon})\,\mathcal{F}_1 + (\vec{\sigma}\cdot\hat{q})\,(\vec{\sigma}\times\hat{k})\cdot\hat{\epsilon}\,\mathcal{F}_2$$
$$+i\,(\hat{\epsilon}\cdot\hat{q})\,(\vec{\sigma}\cdot\hat{k})\mathcal{F}_3 + i(\hat{\epsilon}\cdot\hat{q})(\vec{\sigma}\cdot\hat{q})\,\mathcal{F}_4$$

require 8 “properly chosen” experiments to reconstruct the amplitudes (for each bin in energy and angle). No analytic behavior imposed, neither in energy nor in angle.

Instead: expansion of $\mathcal{F}_i$ in Legendre polynomials of finite order, e.g. $L = 0, 1, 2$.

Omalenko (1981) and Wunderlich *et al.*:

Four quantities need to be known (or more to resolve discrete ambiguities).

4.2 Measurable quantities, and measured ones

$$\begin{aligned}\sigma = \sigma_0\{1 \quad &- \quad p_\perp \Sigma \cos 2\varphi + t_x \left(-p_\perp H \sin 2\varphi + p_\odot F\right) \\ &- \quad t_y \left(-T + p_\perp P \cos 2\varphi\right) \\ &- \quad t_z \left(-p_\perp G \sin 2\varphi + p_\odot E\right)\}, \qquad \text{BT}\end{aligned}$$

$\sigma_0, \Sigma, T, P,$ $\quad E, F, G, H$: **8 variables measured!**

But not "properly chosen." No direct reconstruction of CGLN amplitudes.

However, a truncated partial wave expansion yields a unique solution!

$$\begin{aligned}\sigma = \sigma_0\{1 \quad &- \quad p_\perp \Sigma \cos 2\varphi + \sigma_{x'} \left(-p_\perp O_{x'} \sin 2\varphi - p_\odot C_{x'}\right) \\ &- \quad \sigma_{y'} \left(-P + p_\perp T \cos 2\varphi\right) \\ &- \quad \sigma_{z'} \left(p_\perp O_{z'} \sin 2\varphi + p_\odot C_{z'}\right)\}, \qquad \text{BR} \\ \sigma = \sigma_0\{1 \quad &+ \quad \sigma_{y'} P + t_x \left(\sigma_{x'} T_{x'} + \sigma_{z'} T_{z'}\right) \\ &+ \quad t_y \left(T + \sigma_{y'} \Sigma\right) \\ &- \quad t_z \left(\sigma_{x'} L_{x'} - \sigma_{z'} L_{z'}\right)\} . \qquad \text{TR}\end{aligned}$$

4.3 Energy independent fits with $L = 0, 1, 2$

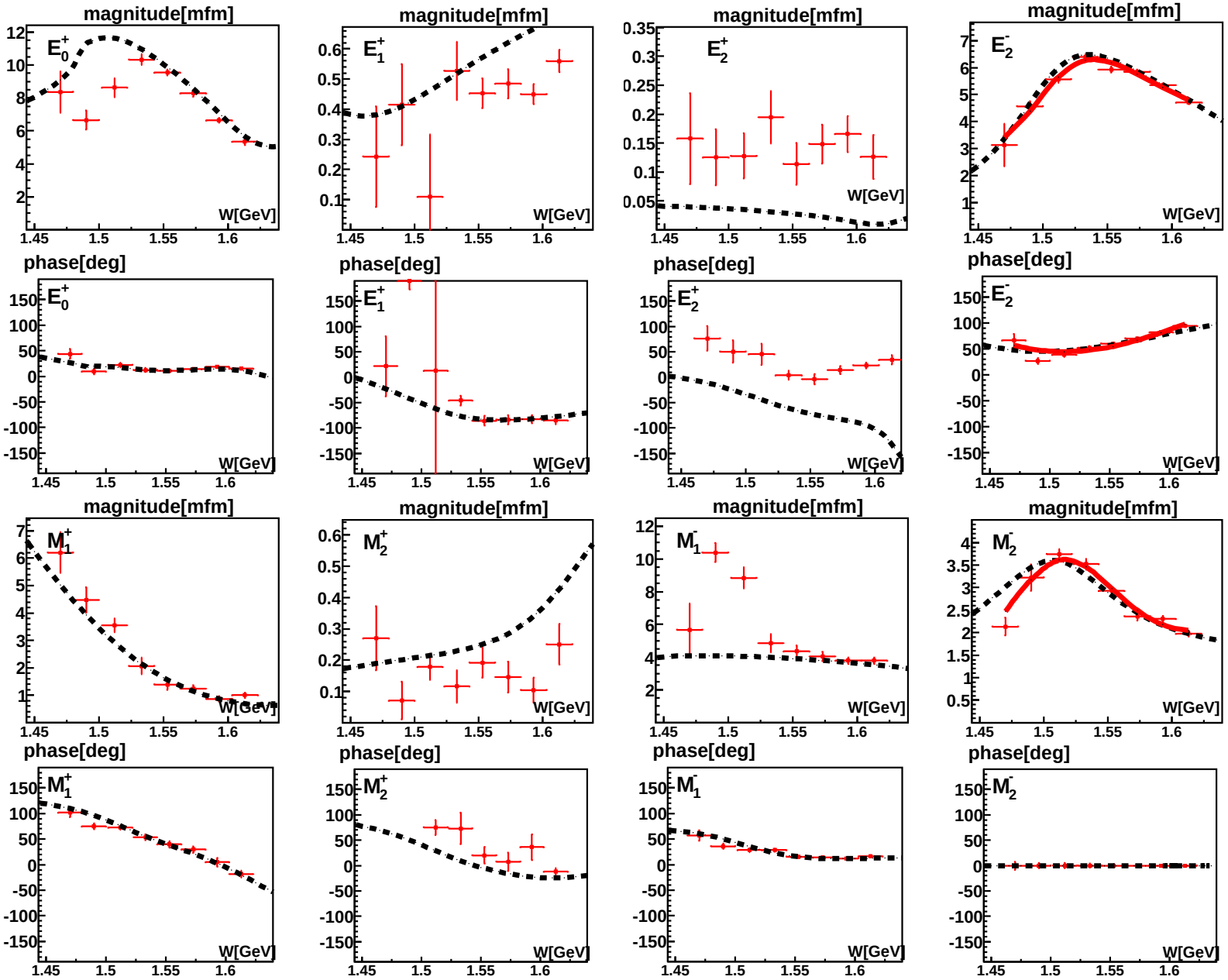

4.4 What causes the peak in S_{11} and the dip in P_{11} ?

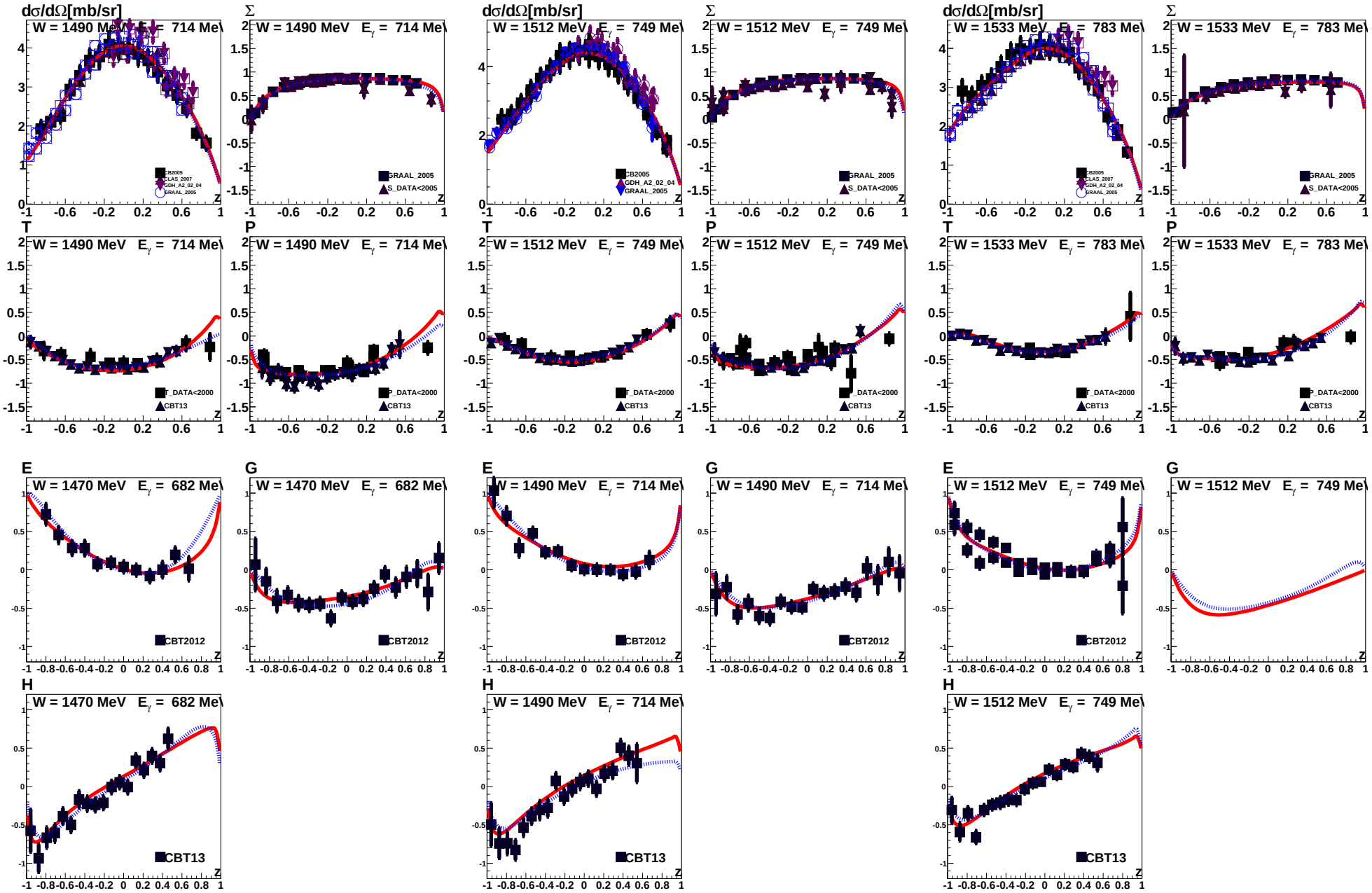

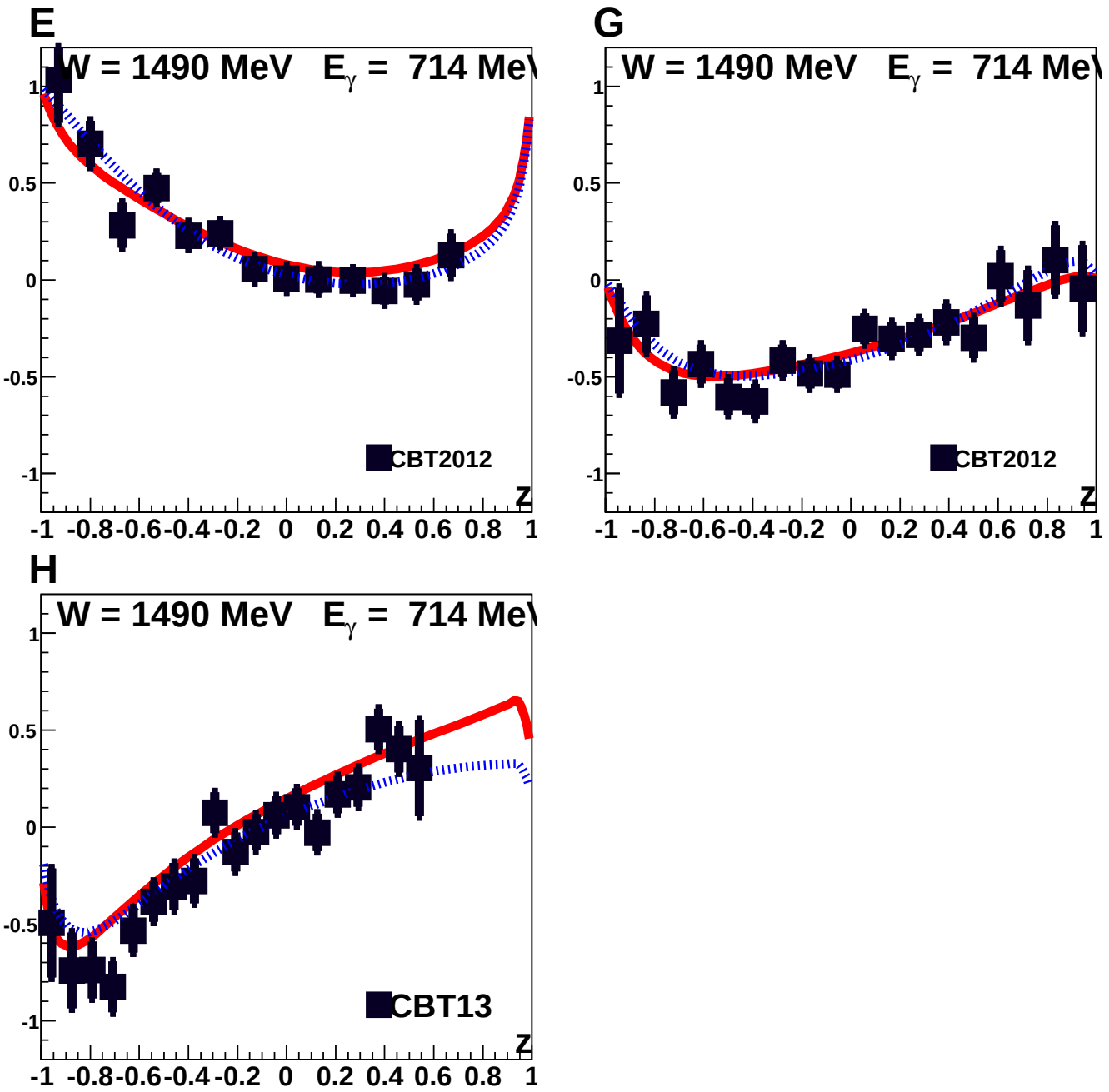
E
W = 1490 MeV E$_\gamma$ = 714 MeV
CBT2012
z
G
W = 1490 MeV E$_\gamma$ = 714 MeV
CBT2012
z
H
W = 1490 MeV E$_\gamma$ = 714 MeV
CBT13
z
1
0.5
0
-0.5
-1
-1 -0.8 -0.6 -0.4 -0.2 0 0.2 0.4 0.6 0.8 1

4.5 Results

1. Energy-independent analysis converges to a unique solution
2. The solution is often compatible with the energy dependent BnGa analysis
3. Small waves reveal some discrepancies
4. Two points in the E_0^+ and M_1^+ have a significant problem
5. The helicity amplitude of $N(1520)3/2^-$ (D_{13}) can be determined:

	$A_{1/2}$	$A_{3/2}$
Energy independent	-0.030±0.009	0.114±0.013
Energy dependent	-0.022±0.004	0.131±0.010

5 Conclusions

- Amplitudes for the reaction $\pi^- p \to \Lambda K^0$ have been reconstructed.
- Without data on R, A or β, a (truncated) energy independent analysis on data on $\pi^- p \to \Lambda K^0$ leads to ambiguities
- The resulting amplitudes (real and imaginary part) are often presented as points with error bars. These look like “experimental” data but they are not!
- A truncated energy independent partial wave analysis has been performed on the reaction $\gamma p \to p\pi^0$ for $1.46 < W < 1.62$:

  - amplitudes with magnitudes smaller than 1 in this range were frozen to the values derived from an energy-dependent fit BnGa2013
  - there is “crosstalk” between the E_0^+ and M_1^- amplitudes.
  - The energy independent E_0^+ and M_1^- amplitudes should not be used for a fit!

- - The E_2^- and M_2^- amplitudes can be fitted; the fit returns helicity amplitudes for the photo-excitation of $N(1520)3/2^-$ compatible with prior knowledge.

Ambiguities:

$$f(W,z) = \frac{1}{\sqrt{qk}} \sum_{l=0}^{L} \left[(l+1) A_l^+(W) + l A_l^-(W) \right] P_l(z) \ ,$$

$$g(W,z) = \frac{1}{\sqrt{qk}} \sin\Theta \sum_{l=1}^{L} \left[A_l^+(W) - A_l^-(W) \right] P_l'(z) \ . \tag{3}$$

$$(1 \pm P) \frac{d\sigma}{d\Omega} = |f \pm ig|^2 . \tag{4}$$

Idea:

Replace the two functions $(1 \pm P)\frac{d\sigma}{d\Omega}$ by a single function by expanding the physical region of the scattering angle Θ from $[0, \pi]$ to $[0, 2\pi]$ and introducing a new variable $w = e^{i\Theta}$.

Now: the f amplitude is even in power of w and w^{-1} since it depends on $z = \frac{1}{2}(w + w^{-1})$.

The g amplitude contains $\sin\Theta = \frac{1}{2i}(w - w^{-1})$ and so behaves as

$$g(w^{-1}) = -g(w).$$

We define the function

$$F(w) = f(w) + ig(w)\,. \tag{5}$$

For $\Theta\,\epsilon\,[0, \pi]$

$$F(w) = f(z) + ig(z)\ , \quad |F(w)|^2 = (1 + P)\frac{d\sigma}{d\Omega} \tag{6}$$

For $\Theta\,\epsilon\,[\pi, 2\pi], \sin\Theta < 0$ **and** $g(w) = -g(z)$**, hence**

$$F(w) = f(z) - ig(z)\ , \quad |F(w)|^2 = (1 - P)\frac{d\sigma}{d\Omega}\,. \tag{7}$$

Let us rewrite $|F(w)|^2$ **as a power series in** w**:**

$$|F(w)|^2 = \sum_{n=-N}^{N} a_n w^n \tag{8}$$

where N **depends on maximal orbital momentum** L **in eq. (3). Since** $|F(w)|^2$ **is real on the unit circle in the** w**-plane, we can write this function as a product of roots in the**

following form

$$|F(w)|^2 = C \prod_{i=1}^{N} (w - w_i)(w^{-1} - w_i^*) \,. \tag{9}$$

$w^* = w^{-1}$ on the unit circle. Thus

$$F(w) = C^{\frac{1}{2}} e^{i\phi} \prod_{i=1}^{N} (w - w_i) \,. \tag{10}$$

Equation (10) is not the only possible solution, one can as well take $(w - w_i)$ or $(w^{-1} - w_i^*)$ as a root, and this gives 2^N different solutions. But not all of these solution are physically sensible. In the next section we discuss the ambiguities in the case when only a limited number of amplitudes are taken into account.